

Melatonin's Protective Effects on Neurons in an *in Vitro* Cell Injury Model

Wei Gu^{1,†}, Mimi Wu^{1,†}, Shihe Cui¹, Jinhua Bo^{1,*}, Hao Wu^{1,*}

¹Department of Anesthesiology, Nanjing Drum Tower Hospital, Affiliated Hospital of Medical School, Nanjing University, 210008 Nanjing, Jiangsu, China

*Correspondence: bojinhua@njgly.com (Jinhua Bo); 13813912046@163.com (Hao Wu)

†These authors contributed equally.

Published: 20 March 2024

Background: Currently, the role of melatonin (MT) in neuronal damage remains unclear and this study aimed to explore the protective effects of MT on neurons in an *in vitro* cell injury model.

Methods: The Sprague Dawley (SD) rat traumatic brain injury (TBI) model was prepared, and brain tissue extract (BTE) from the injured area were generated. To establish a cell injury model *in vitro*, the BTE was added to the culture medium during the neuron culture process. MT was introduced into the culture medium of the cell injury model to observe its protective effects on neurons. Relevant molecular biology experiments were conducted to observe cellular oxidative stress status, inflammation, endoplasmic reticulum (ER) stress, mitochondrial damage, and neuronal apoptosis.

Results: When compared to the control group, the BTE group exhibited a significant increase in cellular oxidative stress, inflammation, neurofilament light polypeptide (NEFL) expression, and ER stress. Additionally, the mitochondrial DNA (mtDNA) copy number significantly decreased, and there was a higher count of apoptotic cells ($p < 0.05$). Upon the addition of MT to the culture medium of the *in vitro* cell injury model, there was a significant reduction in cellular oxidative stress, inflammation, and NEFL levels. This addition also mitigated ER stress, increased mtDNA copy numbers, and decreased the ratio of cell apoptosis ($p < 0.05$).

Conclusions: In the *in vitro* cell injury model, MT demonstrates the capacity to inhibit cellular oxidative stress, inflammation, and ER stress levels. Additionally, it diminishes mtDNA damage, fosters cell viability, and serves as a protective agent against both apoptosis and necrosis in neurons.

Keywords: traumatic brain injury; melatonin; neurons; apoptosis

Introduction

Traumatic brain injury (TBI) denotes brain dysfunction resulting from external forces impacting or injuring the head [1]. It stands as a prevalent cause of disability and mortality worldwide. Occupations with high risk, traffic accidents, sports activities, warfare, violence, and falls represent common causes of TBI [1,2]. Current treatments for TBI encompass first aid, surgical interventions, medication, and rehabilitation. The exploration of neuroprotective drugs for TBI remains an active area of research aimed at fostering brain tissue repair and mitigating post-injury neural dysfunction [1,3]. These drugs encompass herbal medicines, peptide-based medications, adrenergic receptor agonists, and vitamins [2,4–6]. However, no specific neuroprotective drug is universally adopted for TBI treatment. Research into neuroprotective drugs remains at an early stage, necessitating further clinical trials and studies to validate their safety and efficacy.

Melatonin (MT) is a hormone produced by the pineal gland, displaying multiple biological effects. It serves to regulate biological rhythms, acts as an antioxidant, modulates immune function, exhibits anti-inflammatory properties, and demonstrates potential anticancer effects [7–9]. Furthermore, MT is associated with neuroprotection, cardiovascular health, reproductive system function, and cognitive function. Ongoing research is actively exploring these areas [10,11]. The diverse biological effects of MT play crucial roles in numerous physiological processes [7]. Some experiments have investigated the potential therapeutic role of melatonin as a neuroprotective agent in preventing neurodegeneration subsequent to TBI, particularly focusing on memory and cognitive impairment [12,13]. While the impact of MT on TBI seems primarily mediated through indirect mechanisms, involving the modulation of inflammatory processes, MT may also alter specific mechanisms [14]. This study aims to delve into the neuroprotective effects of melatonin using an *in vitro* cell injury model and uncover its potential underlying mechanisms.

Methods

TBI Rat Model Preparation

Three male Sprague Dawley (SD) rats (220–250 g) were procured from the Animal Experimental Center of Nanjing Hospital Affiliated to Nanjing Medical University. The TBI rat model was established utilizing a modified Feeney free-fall method [15]. Following intraperitoneal anesthesia using 2% sodium pentobarbital (2 mL/kg, 4390-16-3, Sigma, Darmstadt, Germany), the rats were secured in a stereotaxic device, and their heads underwent routine disinfection. Subsequently, a 5 mm diameter bone window was created approximately 2.5 mm posterior to the coronal suture and 2.5 mm to the left of the sagittal suture. This procedure exposed the dura mater, allowing for impact-induced TBI on the brain tissue through the bone window using a freely dropped weight (40 g) released through a copper tube from a height of 15 cm. Once impact occurred, the weight was promptly removed, hemostasis was achieved, and the bone window was sealed with bone wax followed by skin suturing.

Brain Tissue Extract (BTE) Preparation

Three days post TBI, rats were euthanized by intraperitoneal injection of sodium pentobarbital (100 mg/kg, 4390-16-3, Sigma, Darmstadt, Germany). Subsequently, the skull was opened, and injured brain tissue was extracted and weighed. The tissue was then placed in a sterile grinder, with the addition of 1 milliliter of basal culture medium per every 100 grams of brain tissue. After grinding the tissue thoroughly for 5 minutes, it was allowed to settle for an additional 5 minutes. Following this, high-speed centrifugation at 12,000 rpm for 15 minutes was performed. The resulting supernatant was collected and stored in a –80 °C freezer for future use.

Determination of Half Maximal Inhibitory Concentration (IC₅₀) of BTE

Primary rat embryonic cortical neurons were procured from ThermoFisher (A1084001, ThermoFisher, Waltham, MA, USA) and seeded in 24-well culture plates at a concentration of 1×10^5 cells/mL using DMEM/F12 medium (11320033, ThermoFisher, Waltham, MA, USA). Neuronal morphology and marker detection were depicted in the control group of Fig. 5, revealing approximately 98% positivity for microtubule-associated protein 2 (MAP2), a neuronal marker. The experimental groups were categorized as follows: control group (DMEM/F12 medium), brain tissue extract (BTE) 15 μ L/mL group, BTE 30 μ L/mL group, BTE 60 μ L/mL group, BTE 120 μ L/mL group, and BTE 240 μ L/mL group, each containing the specified amount of BTE in the DMEM/F12 medium. All cells were incubated at 37 °C in an environment with 5% CO₂, 95% air, and saturated humidity for 48 hours. Hoechst fluorescent staining did not reveal any mycoplasma in-

fection (Fig. 1A). Subsequently, cell viability was assessed using the 3-(4,5)-dimethylthiazolium (-z-y1)-3,5-diphenyltetrazolium bromide (MTT) kit (C0009S, Beyotime, Haimen, China). The optical density (OD) of each well was measured at a wavelength of 570 nm utilizing a microplate reader (ELX800, BioTek, Winooski, VT, USA). The percentage inhibition rate of cell viability was calculated as (control group OD value – OD value of each group)/control group OD value \times 100%. The half maximal inhibitory concentration (IC₅₀) was determined to be 55.08 μ L/mL through Probit regression analysis. For the subsequent experiment, a concentration of 55 μ L/mL was chosen.

Determination of Concentration for 50% of Maximal Effect (EC₅₀) of MT

Primary rat embryonic cortical neurons were allocated into various groups: the control group (DMEM/F12 medium) and MT treatment groups, including MT 10 nmol/L, MT 20 nmol/L, MT 40 nmol/L, MT 80 nmol/L, and MT 160 nmol/L. Each group contained DMEM/F12 medium supplemented with 55 μ L/mL BTE and the specified concentration of MT (ST1497-1g, Beyotime, Haimen, China). All cells were cultured at 37 °C in an environment with 5% CO₂, 95% air, and saturated humidity for 48 hours. Hoechst fluorescent staining did not reveal any mycoplasma infection (Fig. 1B). Subsequently, cell viability was assessed using the MTT kit (C0009S, Beyotime, Haimen, China). The OD of each well was measured at a wavelength of 570 nm with a microplate reader (ELX800, BioTek, Winooski, VT, USA). The percentage protection rate of cell viability was calculated as (OD value of each group – control group OD value)/control group OD value \times 100%. The concentration for 50% of maximal effect (EC₅₀) was calculated to be 122.11 nmol/L using Probit regression analysis. For subsequent experiments, a concentration of 120 nmol/L was chosen.

Cell Injury Model Preparation and MT Treatment

The primary rat embryonic cortical neurons were categorized into distinct groups: the control group (DMEM/F12 medium), the BTE group (DMEM/F12 medium containing 55 μ L/mL BTE), the MT group (DMEM/F12 medium containing 55 μ L/mL BTE and 120 nmol/L MT), and the Solvent group (DMEM/F12 medium containing 55 μ L/mL BTE and an equivalent volume of normal saline (NS)). All cells were incubated at 37 °C in an atmosphere of 5% CO₂, 95% air, and saturated humidity for 72 hours. Subsequently, these cells were utilized in the subsequent experiments.

Cell Viability Assessment

According to the instructions of MTT reagent kits (C0009S, Beyotime, Haimen, China), cell viability was measured in the above-mentioned cell model.

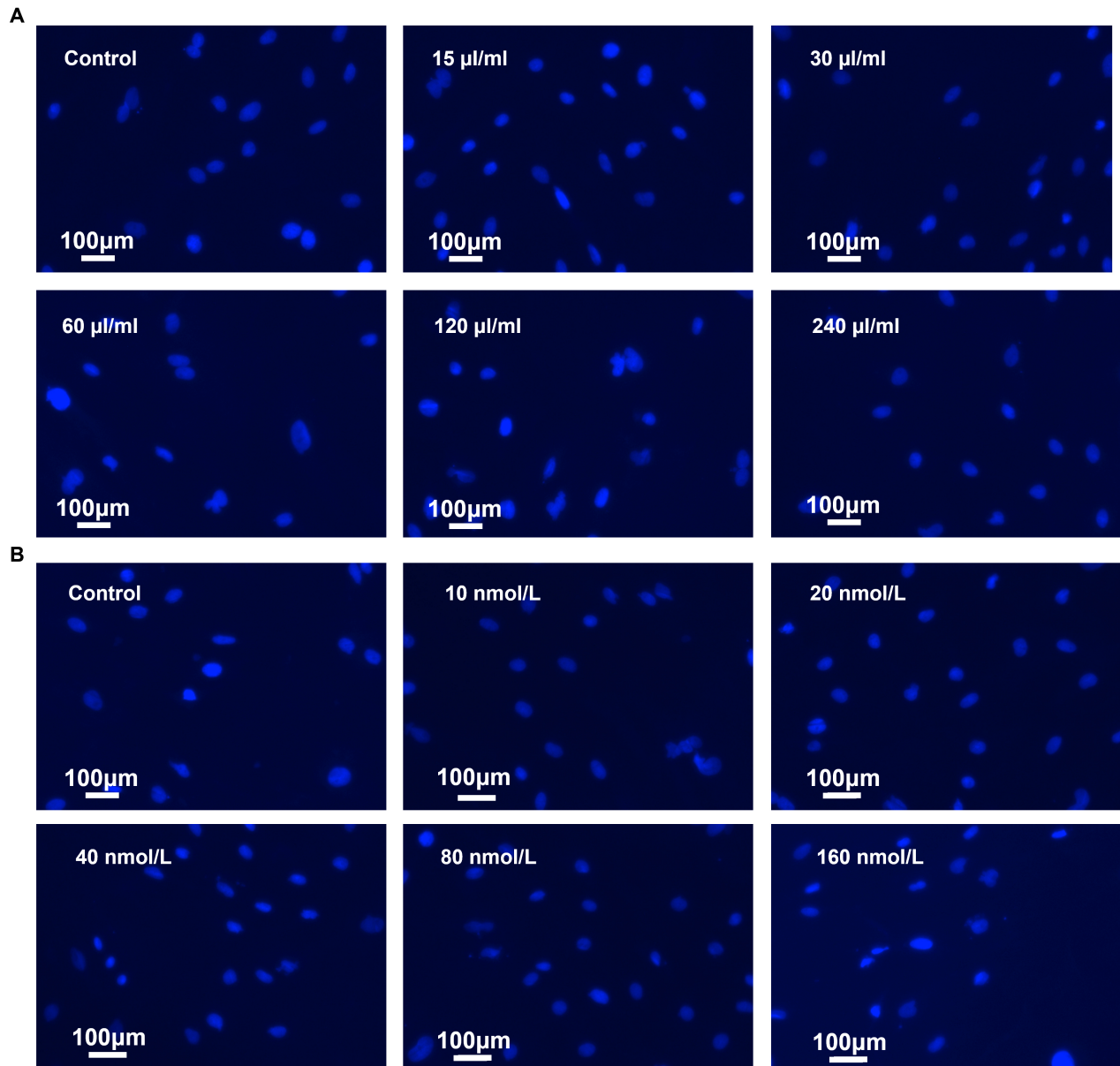


Fig. 1. Hoechst fluorescent staining did not reveal mycoplasma infection. (A) Cell injury model preparation experiment. (B) Melatonin (MT) treatment experiment. Bar = 100 μm .

Cellular Oxidative Stress Status Assessment

According to the instructions of malondialdehyde (MDA) kit (S0131S, Beyotime, Haimen, China) and superoxide dismutase (SOD) reagent kit (S0086, Beyotime, Haimen, China), MDA and SOD levels were measured in the above-mentioned cell model.

Cellular Inflammation Level Assessment

According to the instructions of tumor necrosis factor alpha (TNF- α) enzyme-linked immunosorbent assay (ELISA) kit (ab236712, UK) and Interleukin 10 (IL-10) ELISA kit (ab214566, Abcam, Cambridge, UK), TNF- α and IL-10 levels were measured in the above-mentioned cell model.

Cellular Endoplasmic Reticulum (ER) Stress Status Assessment

The culture medium of each group was replaced with DMEM medium containing 3 $\mu\text{mol/L}$ Fura-2/AM (ab120873, Abcam, Cambridge, UK). Subsequently, the cells were incubated in a water bath at 37 $^{\circ}\text{C}$ for 0.5 hours and then washed three times with PBS. Fluorescence intensity was measured using an emission wavelength of 510 nm, with excitation wavelengths set at 340 nm and 380 nm. The determination of intracellular calcium levels relied on the ratio of excitation intensities at 340 nm and 380 nm wavelengths.

Cellular mtDNA Damage Assessment

The mitochondrial NADH dehydrogenase 1 (ND1) copy number was determined using qPCR to evaluate the state of mitochondrial DNA (mtDNA) damage. Genomic DNA from the cells was extracted utilizing a DNA extraction kit (D006, Beyotime, Haimen, China). Subsequently, qPCR amplification was conducted following the instructions outlined in the BeyoRT™ SYBR Green qPCR Mix kit (D7509M, Beyotime, Haimen, China). The reaction system comprised 10 µl of BeyoFast™ SYBR Green qPCR Mix (2X), 2 µL of Forward and Reverse Primer Mix (3 µM), 25 ng of DNA, and 6 µL of RNase-Free ddH₂O, with a total volume of 20 µL. The reaction conditions were set as follows: an initial denaturation at 95 °C for 2 minutes, followed by 40 cycles of denaturation at 95 °C for 15 seconds, and annealing/extension at 60 °C for 15 seconds. The primer sequences used were as follows: mitochondrial ND1: sense 5'-TGAATCCGAGCATCCTACC-3', antisense 5'-ATTCCTGCTAGGAAAATTGG-3'; apolipoprotein B (APOB): sense 5'-CGTGGGCTCCAGCATTCTA-3', antisense 5'-TCACCAGTCATTTCTGCCTTTG-3'. APOB served as an internal reference, and the relative copy number of mtDNA was calculated using the $2^{-\Delta\Delta Ct}$ method.

The Detection of Neuronal Morphology and Quantity

The detection of neuronal morphology and quantity was performed using MAP-2 immunofluorescence. Initially, cells were incubated with the primary antibody, rabbit anti-MAP-2 (1:600, ab5392, Abcam, Cambridge, UK), at 4 °C for 12 hours. Following this, the cells underwent three washes with PBS. Subsequently, incubation with the secondary antibody, Alexa Fluor® 488 goat anti-rabbit IgG (1:1000, ab150077, Abcam, Cambridge, UK) was carried out in a darkroom at room temperature for 4 hours. Post-secondary antibody incubation, the cells were subjected to three PBS washes. For nuclear staining, Hoechst (1:3000) was utilized and applied at room temperature in a darkroom for 30 minutes. Finally, the observation of neurons was conducted under a fluorescence microscope subsequent to mounting with anti-fade mounting medium.

Neuronal Damage Assessment

Neuronal damage was evaluated using the neurofilament light polypeptide (NEFL) ELISA kit (ab288182, Abcam, Cambridge, UK) and the terminal deoxynucleotidyl transferase dUTP nick end labeling (TUNEL) kit (C1089, Beyotime, Haimen, China) following their respective instructions. Culture media were collected for NEFL detection, while cells were used for TUNEL detection. For the TUNEL assay, following detection, cell nuclei were stained with Hoechst (1:3000, C1017, Beyotime, Haimen, China) at room temperature in a darkroom for 30 minutes. Finally,

apoptotic cells were observed using a fluorescence microscope after mounting with anti-fade mounting medium.

Statistical Processing

The metric data obtained underwent the Kolmogorov-Smirnov test using SPSS 21.0 software (IBM Corp., Chicago, IL, USA), revealing a normal distribution. The data were presented as mean ± SD. Intergroup comparisons were performed using one-way analysis of variance (ANOVA). Statistical graphs were created using GraphPad Prism 7.0 (Dotmatics, Boston, MA, USA). Statistical significance was considered when $p < 0.05$.

Results

IC₅₀ of BTE and EC₅₀ of MT

In the *in vitro* setting, neurons were exposed to varying concentrations of BTE (15 µL/mL, 30 µL/mL, 60 µL/mL, 120 µL/mL, and 240 µL/mL). The MTT assay revealed that the inhibitory rate of cell viability was approximately 16.63% at 15 µL/mL BTE. This inhibitory rate notably escalated at 30 µL/mL ($p < 0.05$). Further increases in the concentration (60 µL/mL, 120 µL/mL, and 240 µL/mL) resulted in peak inhibitory rates of cell viability ($p < 0.05$) (Fig. 2A). Probit regression analysis determined an IC₅₀ value of 55.08 µL/mL for BTE, and consequently, a concentration of 55 µL/mL was chosen for subsequent experiments. Following this, in the same *in vitro* setup, neurons were exposed to 55 µL/mL BTE along with varying concentrations of MT (10 nmol/L, 20 nmol/L, 40 nmol/L, 80 nmol/L, and 160 nmol/L). The MTT assay exhibited that the protective rate of cell viability was approximately 15.56% at 10 nmol/L MT. This protective rate exhibited a gradual increase with concentrations of 20 nmol/L and 40 nmol/L ($p < 0.05$). The protective rates of cell viability peaked at concentrations of 80 nmol/L and 160 nmol/L ($p < 0.05$) (Fig. 2B). Probit regression analysis revealed an EC₅₀ value of 122.11 nmol/L for MT, leading to the selection of a concentration of 120 nmol/L for subsequent experiments.

The Protective Effect of MT on Neurons Viability

The MTT assay results indicated a notable reduction in neuronal viability when either BTE alone or BTE along with NS was introduced into the culture medium compared to the control group ($p < 0.05$). Furthermore, neuronal activity exhibited a significant increase upon simultaneous addition of BTE and MT to the culture medium; however, it did not attain the level observed in the control group ($p < 0.05$) (Fig. 3A).

MT Reduced Cellular Oxidative Stress, Inflammation, and ER Stress

Compared to the control group, the levels of MDA, TNF- α , and intracellular calcium demonstrated a significant increase upon the addition of BTE or BTE in combi-

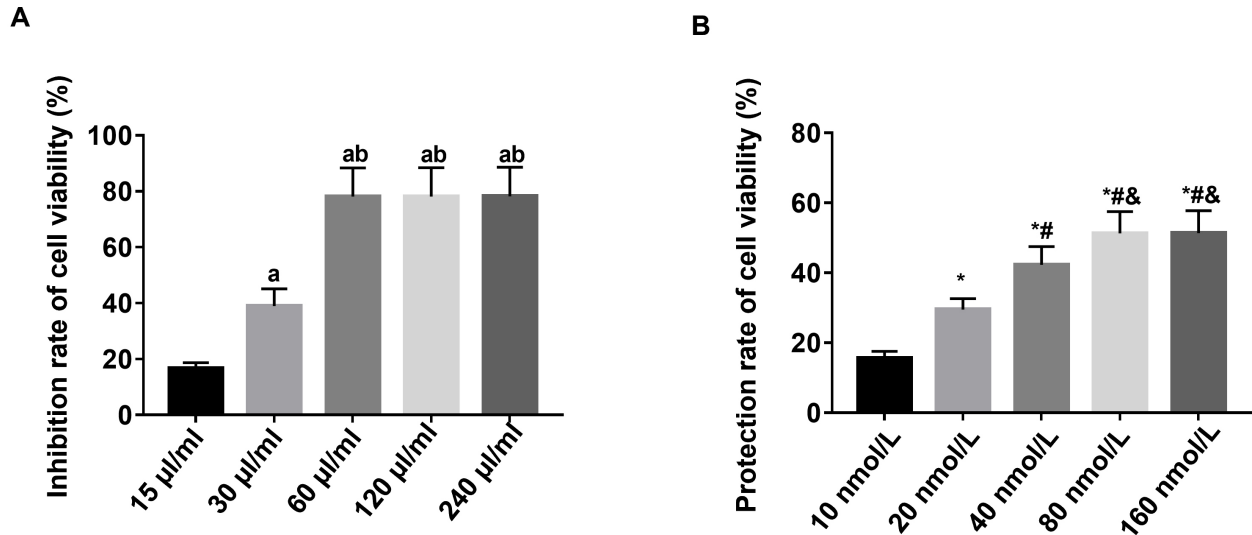


Fig. 2. IC50 of BTE and EC50 of MT. (A) The inhibitory rate of cell viability by was assessed with MTT and the IC50 of BTE was 55.08 μL/mL. a vs.15 μL/mL group, $p < 0.05$; b vs.30 μL/mL group, $p < 0.05$. (B) The protective rate of cell viability of MT was assessed with MTT and the EC50 of MT was 122.11 nmol/L. * vs. 10 nmol/L group, $p < 0.05$; # vs. 20 nmol/L group, $p < 0.05$; & vs. 40 nmol/L group, $p < 0.05$. n = 8. IC50, half maximal inhibitory concentration; BTE, brain tissue extract; EC50, concentration for 50% of maximal effect; MT, melatonin; MTT, 3-(4,5)-dimethylthiaziazolo (-z-y1)-3,5-di-phenyltetrazoliumromide.

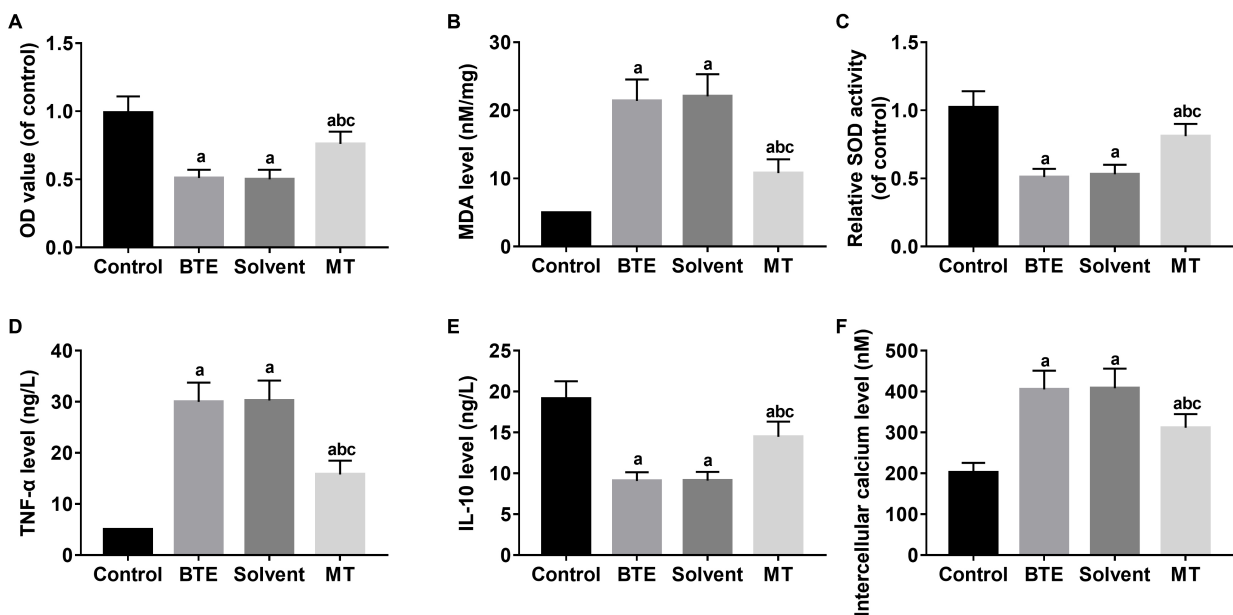


Fig. 3. Cellular activity, oxidative stress, inflammatory response, and ER stress. (A) Cellular activity was assessed with MTT. (B,C) Oxidative stress. (D,E) Inflammatory response state was detected by TNF-α and IL-10 levels. (F) ER stress state was assessed with calcium overload. a vs. control group, $p < 0.05$; b vs. BTE group, $p < 0.05$; c vs. solvent group, $p < 0.05$. n = 6. OD, optical density; MDA, malondialdehyde; SOD, superoxide dismutase; TNF-α, tumor necrosis factor alpha; ER, endoplasmic reticulum; IL-10, Interleukin 10.

nation with NS to the culture medium ($p < 0.05$). Conversely, the levels of MDA, TNF-α, and intracellular calcium exhibited a notable decrease upon simultaneous addition of BTE and MT to the culture medium; however, they

did not return to the levels observed in the control group ($p < 0.05$) (Fig. 3B,D,E,F). Additionally, compared to the control group, the level of SOD significantly declined upon the addition of BTE or BTE in combination with NS to the

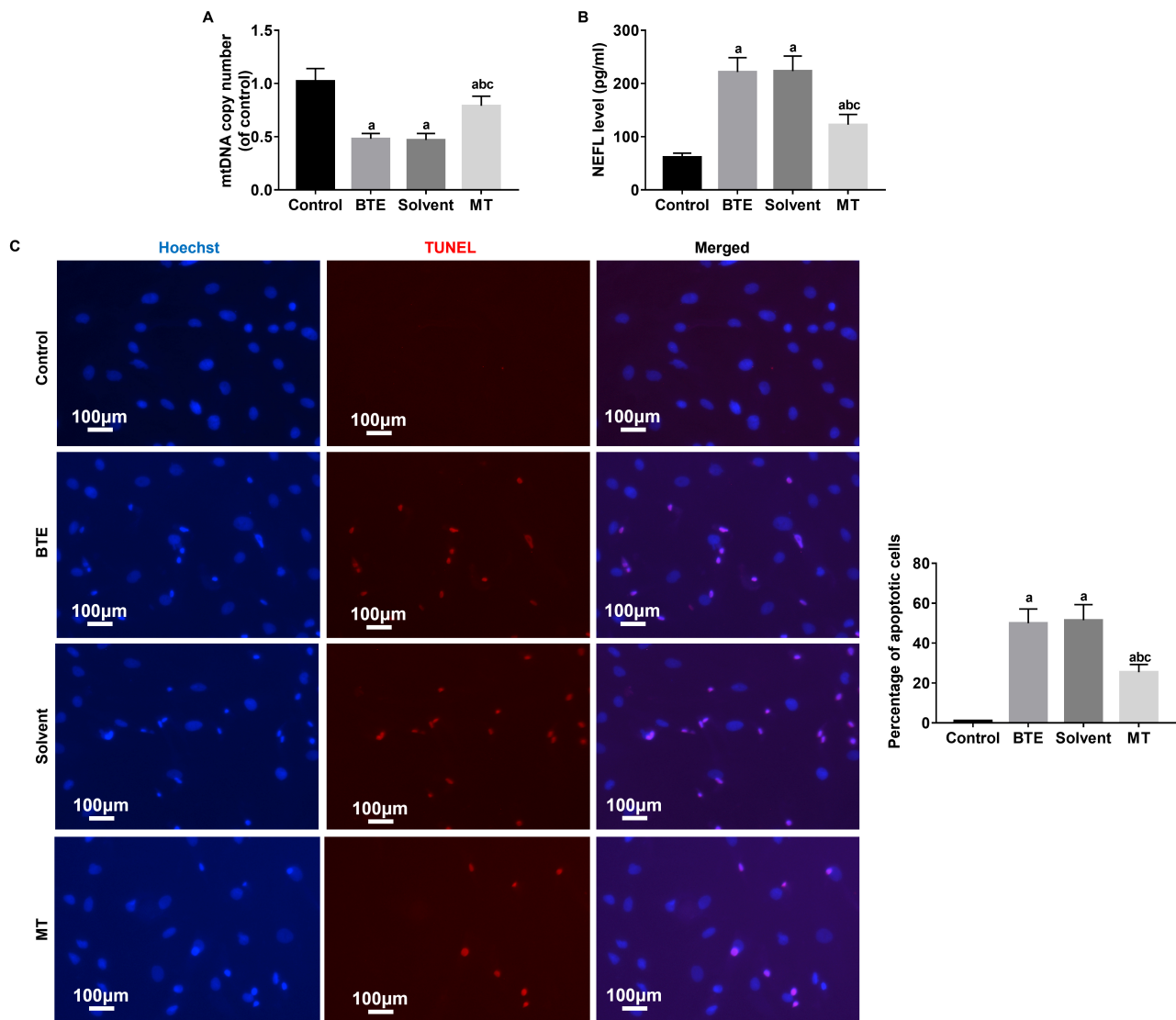


Fig. 4. Cell mitochondria damage, cell apoptosis and necrosis. (A) Cell mitochondria damage was assessed by mtDNA copy number. (B) Cell necrosis was assessed with NEFL level. (C) Cell apoptosis was detected by TUNEL. a vs. control group, $p < 0.05$; b vs. BTE group, $p < 0.05$; c vs. solvent group, $p < 0.05$. Bar = 100 μm . $n = 6$. NEFL, neurofilament light polypeptide; mtDNA, mitochondrial DNA; TUNEL, transferase dUTP nick end labeling.

culture medium ($p < 0.05$). Yet, the SOD level displayed a significant increase upon simultaneous addition of BTE and MT to the culture medium, albeit not reaching the level observed in the control group ($p < 0.05$).

MT Reduced mtDNA Damage

The qPCR results revealed a significant reduction in the copy number of neuronal mtDNA compared to the control group when BTE alone or BTE in combination with NS was added to the culture medium ($p < 0.05$). Notably, the copy number of neuronal mtDNA exhibited a significant increase upon the simultaneous addition of BTE and MT to the culture medium, compared to the BTE and solvent groups. However, it did not reach the level observed in the control group ($p < 0.05$) (Fig. 4A).

MT Reduced Neurons Damage

Compared to the control group, the NEFL level exhibited a significant increase upon the addition of BTE alone or BTE in combination with NS to the culture medium ($p < 0.05$). Conversely, the NEFL level showed a significant decrease upon the simultaneous addition of BTE and MT to the culture medium; however, it did not reach the level observed in the control group ($p < 0.05$) (Fig. 4B). In the control group, only a few apoptotic cells were observed, while a considerable number of apoptotic cells were evident in the BTE and solvent groups ($p < 0.05$). Notably, when cells were treated simultaneously with BTE and MT, the number of apoptotic cells significantly decreased compared to the BTE and solvent groups, although it remained higher than the control group ($p < 0.05$) (Fig. 4C).

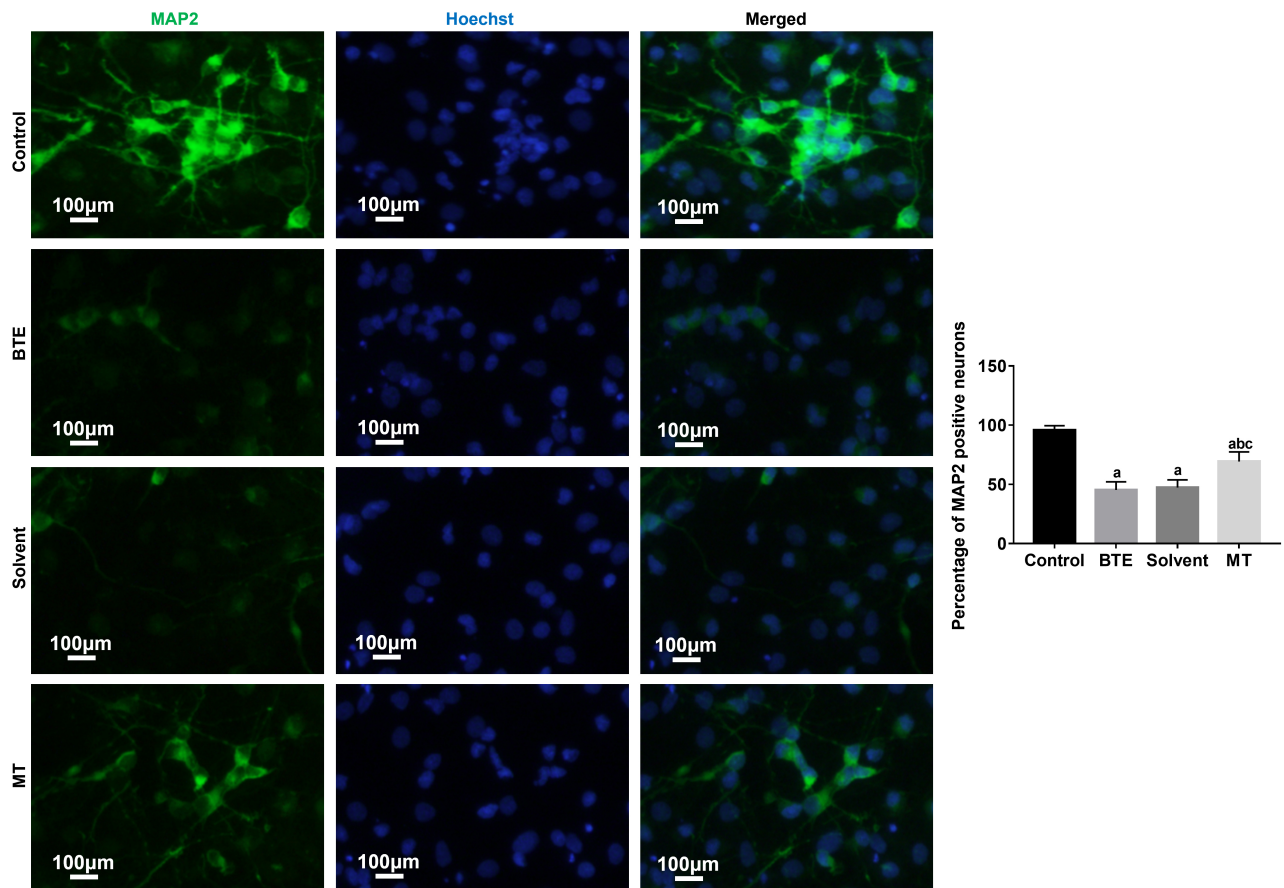


Fig. 5. Neuronal survival was assessed with MAP2 immunofluorescence staining. a vs. control group, $p < 0.05$; b vs. BTE group, $p < 0.05$; c vs. solvent group, $p < 0.05$. Bar = 100 μm . n = 6. MAP2, microtubule-associated protein 2.

Assessment of Neuronal Survival

The immunofluorescence staining results of MAP2 demonstrated that the control group exhibited a substantial number of MAP2-positive neurons characterized by complete cell morphology, abundant and extended dendrites, and intense immunofluorescence. Contrastingly, in the BTE and solvent groups, a reduced number of MAP2-positive neurons were observed, exhibiting diminished fluorescence intensity and fewer dendritic processes. The MT group displayed a moderate quantity of MAP2-positive neurons with acceptable fluorescence intensity and dendritic morphology. Comparing the percentages of MAP2-positive neurons among the groups revealed significant differences. Specifically, in comparison to the control group, the percentage of MAP2-positive neurons significantly declined in the BTE and solvent groups ($p < 0.05$). However, the MT group displayed a significantly higher percentage than the BTE and solvent groups but remained lower than the control group ($p < 0.05$) (Fig. 5).

Discussion

TBI induces not only primary injury but also triggers a sequence of secondary injuries, encompassing a cas-

cade of biological and chemical reactions following the initial trauma, thereby exacerbating damage to brain tissue. Secondary injuries can manifest rapidly within minutes post-trauma or gradually evolve over a span of days or weeks. They commonly encompass brain edema, hypoxia-ischemia, disruption of the blood-brain barrier, and dysfunction in brain metabolism [16,17]. Secondary injuries associated with TBI encompass a multitude of mechanisms that may interplay and intensify damage to brain tissue. These mechanisms include disruptions in energy metabolism, oxidative stress, inflammatory responses, dysregulation of the immune system, endoplasmic reticulum (ER) stress, and culminate in cellular apoptosis and necrosis [18–20]. The convergence of these mechanisms contributes to the complexity of secondary injury in TBI, underscoring the multifaceted nature of its impact on brain tissue.

Oxidative stress constitutes a typical physiological response characterized by an excessive generation of reactive oxygen species (ROS) and other oxidizing agents within cells, disrupting the intracellular equilibrium. Following traumatic brain injury (TBI), the inflammatory response and cellular damage activate various cell types, including macrophages, astrocytes, and endothelial cells, releasing substantial quantities of free radicals. Oxidative stress sub-

sequent to TBI may compromise the efficiency of the intracellular antioxidant defense system, leading to reduced activity of antioxidant enzymes like SOD and Glutathione Peroxidase (GPx). This heightened oxidative stress can trigger lipid oxidation reactions, causing damage to lipid molecules and the formation of oxidative lipid products [21]. In the *in vitro* cell injury model utilized in this study, the addition of BTE to the culture medium resulted in a decrease in neuronal SOD levels and a significant increase in MDA levels, indicating an oxidative stress state within the cell model. Neurons, under certain pathological conditions, can generate and release inflammatory factors such as cytokines (e.g., TNF- α , Interleukin-1 β (IL-1 β), etc.), which contribute to neuroinflammatory responses and the progression of diseases [22]. Inflammatory inhibitory factors, such as IL-10, possess anti-inflammatory properties and can suppress the activity of various inflammatory cells, thereby mitigating inflammatory reactions [23]. In the cell injury model employed in this study, the addition of BTE to the culture medium resulted in a decrease in IL-10 levels and a significant increase in TNF- α levels in neurons. After TBI, the excessive production of ROS and disrupted regulation of calcium ions within cells can induce endoplasmic reticulum (ER) stress [24]. In this study, the addition of BTE to the culture medium induced pronounced intracellular calcium overload in neurons, suggesting an ER stress state in the cell model. Furthermore, the qPCR results revealed a significant decrease in the copy number of neuronal mtDNA after adding BTE to the culture medium, indicating BTE-induced mtDNA damage in neurons. Moreover, the addition of BTE to the culture medium significantly decreased cell viability and the number of neurons, resulting in an elevated number of apoptotic cells and increased NEFL levels. These outcomes collectively suggest that the cell injury model utilized in this study was relatively successful in replicating several key features associated with neuronal injury following exposure to BTE.

Following traumatic brain injury (TBI), a complex interplay exists among oxidative stress, the inflammatory response, endoplasmic reticulum (ER) stress, and mitochondrial DNA damage. Oxidative stress and ER stress can trigger the inflammatory pathway, instigating the release of inflammatory mediators and amplifying the inflammatory reactions. Simultaneously, the inflammatory response itself can generate additional oxidants. Moreover, oxidative stress and ER stress can induce mitochondrial dysfunction, leading to damage in mitochondrial DNA. This damage, in turn, may exacerbate oxidative stress and the inflammatory response, establishing a detrimental cycle that impedes cell and brain injury recovery. A comprehensive understanding and intervention targeting these interconnected mechanisms are crucial for devising novel treatment strategies and facilitating the recovery of individuals with TBI. Post-TBI, melatonin (MT) secretion might decrease, experience disruptions in release rhythm, and interfere with its functional

mechanisms, thereby influencing sleep, inflammatory response, and neuroprotection [25]. In the present study, combining BTE addition to the culture medium with MT treatment significantly mitigated neuronal oxidative stress, inflammatory response, ER stress, and mtDNA damage. Notably, this combined treatment notably enhanced neuronal activity and quantity while reducing cellular injury and apoptosis. These outcomes suggest that MT effectively shields neurons in a cellular injury model, potentially attenuating nervous system damage resulting from TBI. Further investigations could delve into MT's impact on intracellular responses, offering promising avenues for treating and preventing TBI. Nevertheless, additional research is imperative to substantiate and further comprehend this protective effect. Validating and elucidating the underlying mechanisms of MT's neuroprotective role in TBI may pave the way for novel therapeutic interventions in the future.

Conclusions

In summary, within the *in vitro* cell injury model, melatonin (MT) demonstrates the capability to inhibit cellular oxidative stress, inflammation, and endoplasmic reticulum (ER) stress. It also displayed the ability to diminish mtDNA damage, enhance cell viability, and protect neurons from apoptosis and necrosis.

Availability of Data and Materials

The datasets used and/or analyzed during the current study are available from the corresponding authors on reasonable request.

Author Contributions

WG and HW conceived and designed the experiments. WG, MW and JB performed the experiments. HW and SC analyzed the data. WG and JB wrote the paper. HW, MW and SC revised the draft paper. All authors read and approved the final manuscript. All authors have participated sufficiently in the work and agreed to be accountable for all aspects of the work.

Ethics Approval and Consent to Participate

The study was approved by the Institutional Ethics Committee of Nanjing Hospital Affiliated to Nanjing Medical University (Approval No. DWSY-22130259).

Acknowledgment

Not applicable.

Funding

This research received no external funding.

Conflict of Interest

The authors declare no conflict of interest.

References

- [1] Capizzi A, Woo J, Verduzco-Gutierrez M. Traumatic Brain Injury: An Overview of Epidemiology, Pathophysiology, and Medical Management. *The Medical Clinics of North America*. 2020; 104: 213–238.
- [2] Hackenberg K, Unterberg A. Traumatic brain injury. *Nervenarzt*. 2016; 87: 203–216. (In German)
- [3] Khellaf A, Khan DZ, Helmy A. Recent advances in traumatic brain injury. *Journal of Neurology*. 2019; 266: 2878–2889.
- [4] Galgano M, Toshkezi G, Qiu X, Russell T, Chin L, Zhao LR. Traumatic Brain Injury: Current Treatment Strategies and Future Endeavors. *Cell Transplantation*. 2017; 26: 1118–1130.
- [5] Lee SY, Amatya B, Judson R, Truesdale M, Reinhardt JD, Uddin T, *et al*. Clinical practice guidelines for rehabilitation in traumatic brain injury: a critical appraisal. *Brain Injury*. 2019; 33: 1263–1271.
- [6] Cui L, Saeed Y, Li H, Yang J. Regenerative medicine and traumatic brain injury: from stem cell to cell-free therapeutic strategies. *Regenerative Medicine*. 2022; 17: 37–53.
- [7] Claustrat B, Leston J. Melatonin: Physiological effects in humans. *Neuro-Chirurgie*. 2015; 61: 77–84.
- [8] Bhattacharya S, Patel KK, Dehari D, Agrawal AK, Singh S. Melatonin and its ubiquitous anticancer effects. *Molecular and Cellular Biochemistry*. 2019; 462: 133–155.
- [9] Chitimus DM, Popescu MR, Voiculescu SE, Panaitescu AM, Pavel B, Zagrean L, *et al*. Melatonin's Impact on Antioxidative and Anti-Inflammatory Reprogramming in Homeostasis and Disease. *Biomolecules*. 2020; 10: 1211.
- [10] Gunata M, Parlakpınar H, Acet HA. Melatonin: A review of its potential functions and effects on neurological diseases. *Revue Neurologique*. 2020; 176: 148–165.
- [11] Miranda-Riestra A, Estrada-Reyes R, Torres-Sanchez ED, Carreño-García S, Ortiz GG, Benítez-King G. Melatonin: A Neurotrophic Factor? *Molecules (Basel, Switzerland)*. 2022; 27: 7742.
- [12] Rehman SU, Ikram M, Ullah N, Alam SI, Park HY, Badshah H, *et al*. Neurological Enhancement Effects of Melatonin against Brain Injury-Induced Oxidative Stress, Neuroinflammation, and Neurodegeneration via AMPK/CREB Signaling. *Cells*. 2019; 8: 760.
- [13] Gao Y, Wang T, Cheng Y, Wu Y, Zhu L, Gu Z, *et al*. Melatonin ameliorates neurological deficits through MT2/IL-33/ferritin H signaling-mediated inhibition of neuroinflammation and ferroptosis after traumatic brain injury. *Free Radical Biology & Medicine*. 2023; 199: 97–112.
- [14] Blum B, Kaushal S, Khan S, Kim JH, Alvarez Villalba CL. Melatonin in Traumatic Brain Injury and Cognition. *Cureus*. 2021; 13: e17776.
- [15] Gu T, Wang X, Yang H, She XN, Chen KH, Wu T, *et al*. Impacts of electroacupuncture on neurological function and protein expressions of apoptosis-related Cyt-C and Caspase-9 in rats with traumatic brain injury. *Zhongguo Zhen Jiu*. 2020; 40: 749–755. (In Chinese)
- [16] Jha RM, Kochanek PM, Simard JM. Pathophysiology and treatment of cerebral edema in traumatic brain injury. *Neuropharmacology*. 2019; 145: 230–246.
- [17] Sulhan S, Lyon KA, Shapiro LA, Huang JH. Neuroinflammation and blood-brain barrier disruption following traumatic brain injury: Pathophysiology and potential therapeutic targets. *Journal of Neuroscience Research*. 2020; 98: 19–28.
- [18] Thapa K, Khan H, Singh TG, Kaur A. Traumatic Brain Injury: Mechanistic Insight on Pathophysiology and Potential Therapeutic Targets. *Journal of Molecular Neuroscience: MN*. 2021; 71: 1725–1742.
- [19] Kaur P, Sharma S. Recent Advances in Pathophysiology of Traumatic Brain Injury. *Current Neuropharmacology*. 2018; 16: 1224–1238.
- [20] Roberson SW, Patel MB, Dabrowski W, Ely EW, Pakulski C, Kotfis K. Challenges of Delirium Management in Patients with Traumatic Brain Injury: From Pathophysiology to Clinical Practice. *Current Neuropharmacology*. 2021; 19: 1519–1544.
- [21] Fesharaki-Zadeh A. Oxidative Stress in Traumatic Brain Injury. *International Journal of Molecular Sciences*. 2022; 23: 13000.
- [22] Shabab T, Khanabdali R, Moghadamtousi SZ, Kadir HA, Mohan G. Neuroinflammation pathways: a general review. *The International Journal of Neuroscience*. 2017; 127: 624–633.
- [23] Garcia JM, Stillings SA, Leclerc JL, Phillips H, Edwards NJ, Robicsek SA, *et al*. Role of Interleukin-10 in Acute Brain Injuries. *Frontiers in Neurology*. 2017; 8: 244.
- [24] Cansler SM, Evanson NK. Connecting endoplasmic reticulum and oxidative stress to retinal degeneration, TBI, and traumatic optic neuropathy. *Journal of Neuroscience Research*. 2020; 98: 571–574.
- [25] Bell A, Hewins B, Bishop C, Fortin A, Wang J, Creamer JL, *et al*. Traumatic Brain Injury, Sleep, and Melatonin-Intrinsic Changes with Therapeutic Potential. *Clocks & Sleep*. 2023; 5: 177–203.